Specific Ion Effects in Solutions of Globular Proteins: Comparison between Analytical Models and Simulation

ARTICLE *in* THE JOURNAL OF PHYSICAL CHEMISTRY B · JANUARY 2006

Impact Factor: 3.3 · DOI: 10.1021/jp0551869 · Source: PubMed

4 AUTHORS, INCLUDING:

Frederico W Tavares
Federal University of Rio de Janeiro
132 PUBLICATIONS **1,431** CITATIONS
SEE PROFILE

Barry W Ninham
Australian National University
444 PUBLICATIONS **20,785** CITATIONS
SEE PROFILE

Specific Ion Effects in Solutions of Globular Proteins: Comparison between Analytical Models and Simulation

M. Boström,*,† F. W. Tavares,‡ D. Bratko,§ and B. W. Ninham||

Department of Physics and Measurement Technology, Linköping University, SE-581 83 Linköping, Sweden, Escola de Química, Universidade Federal do Rio de Janeiro, Brazil, Department of Chemistry, Virginia Commonwealth University, Richmond, Virginia 23284, and Research School of Physical Sciences and Engineering, Australian National University, Canberra 0200, Australia

Received: September 14, 2005; In Final Form: November 3, 2005

Monte Carlo simulations have been performed for ion distributions outside a single globular macroion and for a pair of macroions, in different salt solutions. The model that we use includes both electrostatic and van der Waals interactions between ions and between ions and macroions. Simulation results are compared with the predictions of the Ornstein−Zernike equation with the hypernetted chain closure approximation and the nonlinear Poisson−Boltzmann equation, both augmented by pertinent van der Waals terms. Ion distributions from analytical approximations are generally very close to the simulation results. This demonstrates that properties that are related to ion distributions in the double layer outside a single interface can to a good approximation be obtained from the Poisson−Boltzmann equation. We also present simulation and integral equation results for the mean force between two globular macroions (with properties corresponding to those of hen-egg-white lysozyme protein at pH 4.3) in different salt solutions. The mean force and potential of mean force between the macroions become more attractive upon increasing the polarizability of the counterions (anions), in qualitative agreement with experiments. We finally show that the deduced second virial coefficients agree quite well with experimental results.

I. Introduction

Precipitation is often used as an initial step in purification of proteins from complex solutions because of its low cost and selectivity.[1] Precipitation and many important bioengineering and biochemical processes[1−2] as well as processes in ceramic suspensions[3] depend on interparticle forces. Lewith and Hofmeister showed in a series of papers during the 1880s that these forces, in blood serum plasma and in hen-egg-white protein solutions, could be manipulated, in a highly ion-specific way, by the addition of different salt solutions. Recent English translations of a few of Hofmeister's publications can be found in ref 4. Depending on the anion, different concentrations were required to precipitate a prescribed concentration of egg white. The salts could be ordered in what is now referred to as a Hofmeister sequence of effectiveness. Solubility experiments[5] and low-angle X-ray scattering[6] have revealed that for pH < pI, where salt anions are counterions, the repulsive double-layer force between two proteins increases in the order NaSCN < NaI < NaCl. In contrast, at higher pH > pI, where anions are co-ions, the forces increase in the order NaCl < NaI < NaSCN.

Ninham and Yaminsky[7] demonstrated that one important reason for the failure of double-layer theory to explain the observed ion specificity was the neglect of ionic dispersion potentials acting between ions and macroions. These potentials that originate from quantum electrodynamic fluctuations must for consistency be included in the theory at the same nonlinear level as the electrostatic potentials. At physiological salt concentrations (around 0.1 M and above), electrostatic potentials become strongly screened and ionic dispersion potentials often dominate the interaction. In a series of papers, we have demonstrated that it is possible to understand the observed ion specificity in a large number of systems when these ionic dispersion potentials are included in the theory. A few examples include the surface tension of electrolytes,[8] double-layer forces,[9−10] protein charges,[11] and electrochemical potentials near surfaces (what we refer to as "surface pH").[12] In the present work, we use Monte Carlo simulations[13−20] to demonstrate how the experimentally observed ion specificity in hen-egg-white lysozyme crystallization can be understood when ionic dispersion potentials acting between ions and the proteins are included into the model of the solution.

The Ornstein−Zernike equation (OZ) with the hypernetted chain closure approximation (HNC) is also applied to study spatial ion−macroion and macroion−macroion correlations in aqueous solutions of ionized globular macroions. In analogy with the modified Poisson−Boltzmann approximation,[20b] this approach adequately incorporates the correlations between simple ions and also enables calculations of the effective intermacroion interaction. Successful applications of the hypernetted chain approximation to multicomponent primitive model asymmetric electrolytes have been reported in earlier studies.[21b,22−25]

In the absence of ionic dispersion potentials, Jönsson et al.[13] found good agreement between ion distributions obtained by solving numerically the nonlinear Poisson−Boltzmann equation and from Monte Carlo simulations. Also for a primitive electrolyte model, Bratko et al.[22−25] and Belloni[21b] showed similar results for OZ-HNC integral equations. Below we demonstrate that one obtains equally good agreement between

* Author to whom correspondence should be addressed. E-mail address: mabos@ifm.liu.se.
† Linköping University.
‡ Universidade Federal do Rio de Janeiro.
§ Virginia Commonwealth University.
|| Australian National University.

10.1021/jp0551869 CCC: $30.25
Published on Web 12/06/2005

ion distributions obtained from the two approaches when ionic dispersion potentials are included. This demonstrates that we can use the nonlinear Poisson−Boltzmann equation with confidence to investigate, for example, surface excess to a single interface and other quantities related to ion distributions near a single interface.

We rehearse briefly in section II the theory of the Poisson−Boltzmann equation. The OZ-HNC integral equation and Monte Carlo simulations are outlined in sections III and IV, respectively. We perform a comparison of ion distributions obtained within the three different methods in section V. The mean force between two lysozyme proteins obtained from Monte Carlo simulations and OZ-HNC is presented in section VI. We end with a few concluding remarks in section VII.

II. Poisson−Boltzmann Equation

Near a charged protein, ions experience an electrostatic potential ($\pm e\phi$) that leads to the accumulation (depletion) of counterions (co-ions). According to classical Derjaguin, Landau, Verwey, and Overbeek (DLVO) theory, all monovalent salts should give the same results, and there should be no co-ion adsorption or any significant co-ion surface effects since these ions should be pushed away from the interface. However electrostatic potentials are not the only potentials that influence the ionic distributions near a protein. We let $U_{\pm}(r)$ be the effective interaction potential beyond pure electrostatics experienced by the ions. We include here ionic dispersion potentials acting between ions and between the ions and the interface. There will in general also be contributions from image potentials[14a,b] and solvation energy changes near interfaces and charge groups[14c] and from electrostatic, hard-core, and ionic dispersion interactions between ions and ions and protein charge groups.

The nonretarded dispersion interaction between a point particle and a sphere of radius r_p can be written within the pair summation approximation as

$$U_{\pm} = \frac{B_{\pm}}{(r - r_p)^3[1 + (r - r_p)^3/(2r_p^3)]} \qquad (1)$$

Here the dispersion coefficient ($B_{\pm}$) will be different for different combinations of ions and spherical protein membranes. When retardation is neglected, we can calculate the dispersion coefficients from the corresponding planar interface result as a sum over imaginary frequencies ($i\omega_n = i2\pi k_B T n/\hbar$, where $\hbar$ is Planck's constant).

$$B_{\pm} = \sum_{n=0}^{\infty} \frac{(2 - \delta_{n,0})\alpha^{\pm}(i\omega_n)[\epsilon_w(i\omega_n) - \epsilon_m(i\omega_n)]}{4\beta\epsilon_w(i\omega_n)[\epsilon_w(i\omega_n) + \epsilon_m(i\omega_n)]} \qquad (2)$$

For Na^+, F^-, Cl^-, Br^-, I^-, and SCN^-, the following B values have been used:[10−11] -0.45×10^{-50}, -1.43×10^{-50}, -3.57×10^{-50}, -4.44×10^{-50}, -5.71×10^{-50}, and -10×10^{-50} J m^3. It would be desirable to have a better characterization of the ionic excess polarizabilities and the dielectric properties of membranes and proteins. But although the values presented may deviate slightly from the correct values for a specific ion and a specific protein, they are of the right order of magnitude. Our results are quite general since many proteins (such as lysozyme and cytochrome c) are built up from similar groups and hence have similar dielectric properties in the visible and UV frequency range.

Ion distributions ($c_{\pm}(r)$) and self-consistent electrostatic potentials (ϕ) were obtained numerically by solving self-consistently the nonlinear Poisson−Boltzmann equation[11]

$$\frac{\epsilon_0\epsilon_w}{r^2}\frac{d}{dr}\left(r^2\frac{d\phi}{dr}\right) = -e[z_+ c_+(r) + z_- c_-(r)] \qquad (3)$$

$$c_{\pm}(r) = c\exp(-\beta[z_{\pm}e\phi + U_{\pm}(r)]) \qquad (4)$$

These ion distributions obtained from the Poisson−Boltzmann equation will be compared with ion distributions obtained from Monte Carlo simulations and OZ-HNC.

III. OZ-HNC Integral Equation

Spatial correlation functions of cation−macroion, anion−macroion, and macroion−macroion are determined by solving the multicomponent Ornstein−Zernike equations[27,23] combined with the HNC closure relation. These equations are[28]

$$h_{ij}(r_{ij}) = C_{ij}(r_{ij}) + \sum_k \rho_k \int C_{ik}(r_{ik})h_{jk}(r_{jk})\, d^3r_k \qquad (5)$$

with

$$C_{ij}(r_{ij}) = -u_{ij}(r_{ij})/k_B T + h_{ij}(r_{ij}) - \ln g_{ij}(r_{ij}) \qquad (6)$$

where $h_{ij} = g_{ij} - 1$ is the total correlation function, g_{ij} is the radial distribution function, C_{ij} the direct correlation function, and u_{ij} is the potential interaction between species i and j; ρ_k is the mean number density of species k. In the present paper, the Coulombic pair potential characteristic of the primitive model is augmented by the dispersion van der Waals (short-ranged) interaction between the cation and the macroion and the anion and the macroion. For the pair macroion−macroion, only electrostatic and hard-sphere repulsion interactions are taken into account.

As in previous studies,[22−25] the Rossky−Dale[26] algorithm is used to solve the multicomponent OZ-HNC equations, and numerical details can be found elsewhere.[22−23,27] The cation−macroion and anion−macroion radial distribution functions are directly related to cation and anion concentration profiles near a macroion whereas the logarithm of the macroion−macroion radial distribution function gives the nondimensional potential of mean force between the macroions.

IV. Monte Carlo Simulations

To assess the accuracy of the nonlinear Poisson−Boltzmann equation, we compare its predictions with the results of the OZ-HNC equations and the canonical Monte Carlo simulations for ion concentration profiles near a protein. We also performed calculations of the potential of mean force between two proteins (macroions). In these simulations, dispersion interactions of anion−protein and cation−protein pairs are taken into account by using eq 1. Below we summarize the Monte Carlo simulation procedures, but details are reported elsewhere.[10,15,16]

We first calculated ion concentration profiles near a fixed-charged protein (a macroion with diameter 30 Å) immersed in a dielectric continuum solution. In summary, the cubic simulation box contains a single macroion (protein) and 300 small ions, all with the same diameter (4 Å), that satisfy the overall charge neutrality. The volume of the box is adjusted to give the desired ionic strength. The box size is about an order of magnitude larger than the Debye screening length. Standard canonical Monte Carlo simulation is applied to calculate the

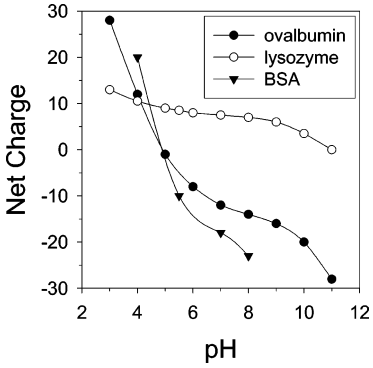

Figure 1. Dependence of the net charge (experimental data) of different proteins on pH. For example, ovalbumin presents $+20\ e^0$ at pH = 3.5 and $-20\ e^0$ at pH = 10. Therefore, Na^+ can be a co-ion or a counterion.

average ion concentrations near the protein. During each run, the protein particle is fixed at the center while small ions are free to move throughout the box. The Ewald-sum method is applied to account for long-range electrostatic interactions. For each simulation, 5×10^6 configurations are used for equilibration. To calculate the average concentrations, 5×10^7 configurations are used.

We then calculated the potential of mean force between two macroions mimicking lysozyme proteins at pH $\approx$ 4.3. The macroions were modeled as hard homogeneously charged ($+10\ e^0$) spheres with an effective diameter of 33 Å. In general, the charge of the protein depends on the particular pH (cf. Figure 1) and salt solution used.[11] In these Monte Carlo simulations, dispersion interactions of ion−ion and ion−macroion pairs are taken into account whereas the term corresponding to the direct dispersion interaction (Hamaker forces) between two macroions is not included because it can always be superimposed to the results we present. The mean force between two macroions surrounded by small ions is hence calculated as a sum of four contributions, the Coulombic forces exerted on either of the macroions by all small ions, the dispersion force exerted on either macroion by all small ions, and the mean force resulting from collisions between hard-sphere macroion particles and small ions. As the box length is about 1 order of magnitude larger than the Debye screening length, the electrostatic interaction between macroions due to the introduction of periodic boundary conditions is negligible. Standard canonical Monte Carlo simulation is applied to calculate the average forces and energies. During each run, the two macroion particles are fixed at a given separation distance *r*, along the box diagonal, while the small ions are free to move throughout the box. The Ewald-sum method is applied to account for long-range electrostatic interactions. It is important to note that the large size of the protein requires that we perform larger simulations compared to those of Tavares et al.[10] This is because there will be a large amount of counterions physisorbed on the protein surface for highly polarizable anions. To have a sufficiently large amount of ions in solution to obtain good statistics, in the two macroion cases we performed simulations with 600 monovalent ions. For each macroion−macroion, we performed 60×10^6 trial moves for equilibration and 120×10^6 for production.

V. Comparison between Ion Distributions Obtained from Monte Carlo Simulations and Poisson−Boltzmann and OZ-HNC Integral Equations

Boström et al.[11] used the Poisson−Boltzmann equation near a charge-regulated sphere to investigate the properties of nearly globular proteins in salt solutions. These calculations revealed

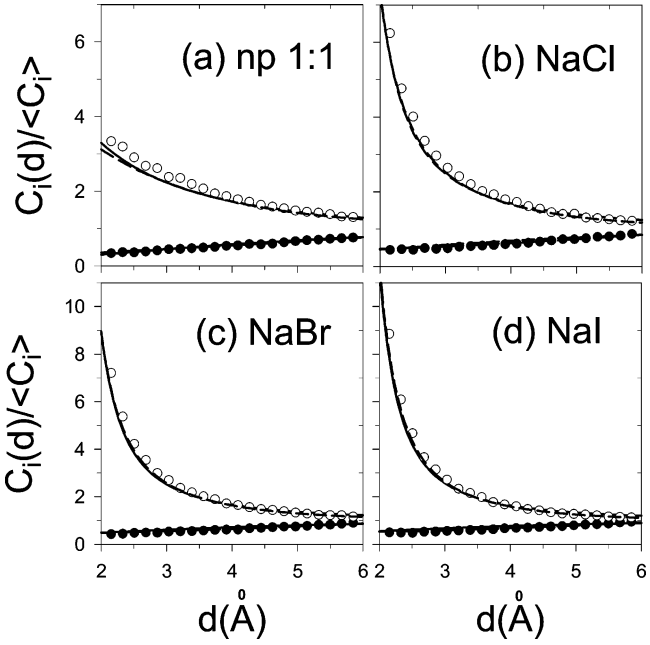

Figure 2. Concentration profiles near a macroion (σ_M = 30 Å and $+20\ e^0$) in a monovalent electrolyte solution of ionic strength 1.0 M, for a salt with nonpolarizable (np) ions, i.e., without van der Waals interaction, and for NaCl, NaBr, and NaI, respectively. Open circles represent counterion concentrations, and dark circles the co-ions. Solid lines are numerical solutions of the nonlinear Poisson−Boltzmann equation, and dashed lines are for the OZ-HNC integral equation.

that ion distributions, surface hydronium concentration, and protein charge all depend on the choice of background salt solution.[11] It is clearly interesting to investigate how well the results obtained with the less time-consuming Poisson−Boltzmann equation compare with the results obtained from Monte Carlo simulations and the OZ-HNC integral equation. For this purpose, we consider a system consisting of a single macroion with constant charge; i.e., we ignore the ion-specific salt dependence of the protein charge. Figure 1 shows the approximate protein charge for three typical proteins as a function of pH. Under typical experimental conditions, bovine serum albumin has a charge that can easily vary between -20 and $+20$ unit charges (e^0). We used Monte Carlo simulations and both the Poisson−Boltzmann and the OZ-HNC integral equations to obtain the ion distributions outside a charged macroion with -20 and $+20\ e^0$ for 1 M nonpolarizable salt ions (np 1:1), NaCl, NaBr, and NaI salt solutions. In the OZ-HNC calculations, the distribution around an isolated macroion was obtained by considering a solution of desired ion concentration and a vanishingly low concentration of macroions. Figures 2 and 3 present results that show very good agreement between ion distributions from the three theoretical methods for monovalent co-ions and counterions. Due to the van der Waals attraction between the couterions and the protein, the concentration of counterions near to the surface is significantly higher than that of nonpolarizable ions at otherwise identical conditions. This behavior cannot be captured by the classical DLVO theory but is adequately described by all three methods we consider, including the nonlinear Poisson−Boltzmann equation with incorporated van der Waals ion−protein potential. The small differences between the Poisson−Boltzmann and OZ-HNC macroion−counterion distributions are related to the neglect of correlations among small ions in the Poisson−Boltzmann approach. These correlations comprise two opposing effects: ion packing, which tends to suppress the concentration of small

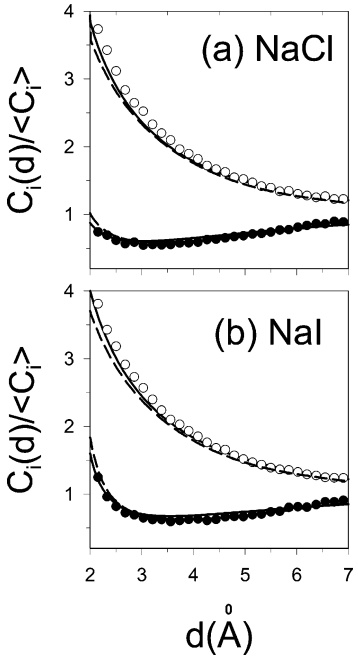

Figure 3. Concentration profiles near a macroion (σ_M = 30 Å and -20 e^0) in a monovalent electrolyte solution of ionic strength 1.0 M for NaCl (a) and NaI (b). Open circles represent counterion concentrations, and dark circles the co-ions. Solid lines are numerical solutions of the nonlinear Poisson−Boltzmann equation, and dashed lines are for the OZ-HNC integral equation.

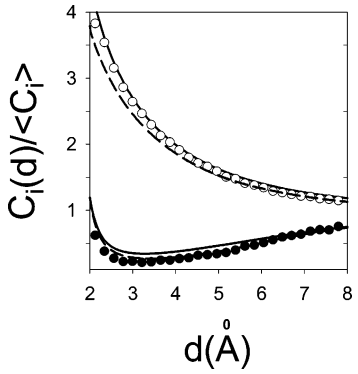

Figure 4. Concentration profiles near a macroion (σ_M = 30 Å and -20 e^0) in solution of ionic strength 1.0 M for Na_2SO_4. Open circles represent counterion concentrations (Na^+), and dark circles the co-ions (sulfate). Solid lines are numerical solutions of the nonlinear Poisson−Boltzmann equation, and dashed lines are for the OZ-HNC integral equation.

ions close to the macroion, and correlated charge density fluctuations, which promote the accumulation of small ions in the double layer, especially in solutions with multivalent ions.

Figures 4 and 5 show concentration profiles near a protein for solutions of Na_2SO_4 with ionic strength equal to 1.0 M. With monovalent counterions and divalent co-ions, we find very good agreement between theory equations and simulation (Figure 4). We note in particular a very good agreement for the predicted co-ion adsorption for highly polarizable divalent anions. It is only when divalent ions are counterions (protein charge $+20$ e^0) that clear deviations occur between the Poisson−Boltzmann equation and both the MC simulation and the OZ-HNC integral equation. In Figure 5, a very high concentration of sulfate is observed, and the Poisson−Boltzmann and HNC equations describe well this behavior. According to the simulation, in this case strong counterion (sulfate) physisorption ("binding") leads to (electrostatic) physisorption of co-ions forming a second layer.

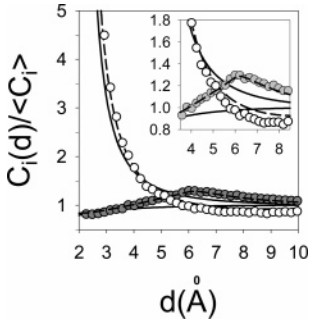

Figure 5. Concentration profiles near a macroion (σ_M = 30 Å and $+20$ e^0) in solution of ionic strength 1.0 M for Na_2SO_4. Open circles represent counterion concentrations (sulfate), and gray circles the co-ions (Na^+). Solid lines are numerical solutions of the nonlinear Poisson−Boltzmann equation, and dashed lines are for the OZ-HNC integral equation. The inside figure shows that the HNC calculations for co-ion distributions coincide with the simulation results.

This maximum characteristic of the second layer is not reproduced by the Poisson−Boltzmann approximation.

This observation is not surprising given the well-known limitations of the Poisson−Boltzmann approximation in describing macroion systems containing multivalent counterions.[13,17b,22−24] Quite generally, the strong ion−ion correlation effects among divalent counterions lead to notable deviations from the predictions of mean-field theories such as the Poisson−Boltzmann approximation, even in the absence of non-Coulombic attractive forces. The reason that the approximation is less severe in cases of multivalent co-ions is that the double layers surrounding the macroions contain no region of strongly elevated co-ion concentration. When short-ranged van der Waals attraction to the macroion is incorporated to the model, strong counterion physisorption ("binding") can lead to physisorption of co-ions forming a second layer. Trial calculations with and without van der Waals forces among small ions show only small differences, indicating that the observed ion layering stems primarily from electrostatic attraction between co-ions and counterions. Apart from this special scenario, the Poisson−Boltzmann approximation augmented by the van der Waals ion−macroion potentials is found quite satisfactory for most scenarios where it performs well in the absence of non-Coulombic attractions. While our comparisons are limited to the distributions around a single macroion, it is safe to generalize the above conclusion to situations involving multiple particles[14,18,19] needed, for example, to estimate inter-macroion potentials of mean force or the osmotic pressure of a colloidal dispersion.

VI. Mean Force and Second Virial Coefficients of Hen-Egg-White Lysozyme.

Using Monte Carlo simulations, Tavares et al.[10] demonstrated that it is possible to obtain the correct trends for second virial coefficients of proteins in salt solutions. As shown below, inclusion of pertinent van der Waals terms can bring predictions of our model into a qualitative agreement with experimental data for the second virial coefficients for hen-egg-white lysozyme in 0.1 M NaCl, 0.2 M NaCl, 0.2 M NaI, and 0.2 M NaSCN solutions. As in the preceding examples (vide supra), the lysozyme protein was modeled as a hard homogeneously charged ($+10$ e^0) sphere with an effective diameter of 33 Å. The specified charge corresponds to a pH of approximately 4.5 whereas it will in depend on the particular pH and salt solution used.[11] We emphasize that our van der Waals parameters have been determined independently from ion polarizabilities[10] and do not serve as adjustable parameters of the model.

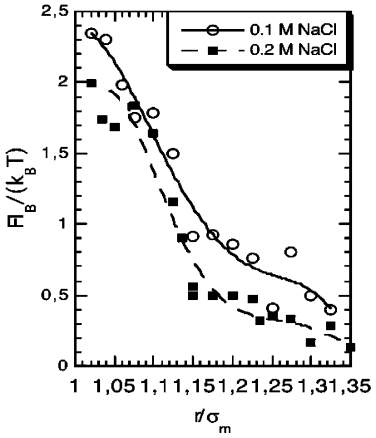

Figure 6. Total mean force (from MC simulations) between two macroions with size and charge corresponding to hen-egg-white lysozyme proteins at pH 4.5 in NaCl electrolytes of ionic strengths 0.1 and 0.2 M. (The lines are fitted curves obtained using KaleidaGraph.)

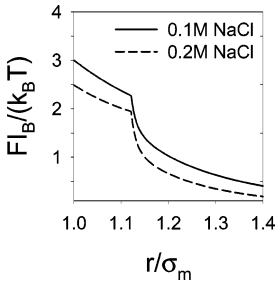

Figure 7. Total mean force between two macroions with size and charge corresponding to hen-egg-white lysozyme proteins at pH 4.5 in NaCl electrolytes of ionic strengths 0.1 and 0.2 M. Lines are numerical solutions of the OZ-HNC integral equation.

Canonical Monte Carlo simulations were used to calculate the mean force $F(r)$ between two macroions in electrolyte solution at a given center-to-center distance r. The potential of mean force (PMF) $W(r)$ is obtained by integration of the mean force: $W(r) = \int_{\infty}^{r} F(r)\, dr$. Details of calculating the PMF from the mean force are given elsewhere.[15,16] We also calculated the potential of mean force and the average force profiles between the macroions from the macroion−macroion radial distribution functions determined using the OZ-HNC integral equation.

Figures 6 and 7 show the effect of salt concentration on the mean force between two lysozyme proteins in 0.1 and 0.2 M NaCl solutions obtained from Monte Carlo simulations and from the OZ-HNC equation, respectively. For clarity of presentation, the direct van der Waals interaction between the two macroions is not included in the force profiles shown in these figures. All forces are normalized using the Bjerrum length, $l_B = e^2/(4\pi\epsilon_0\epsilon k_B T)$, that is at $T = 298$ K around 7.14 Å. From both calculations, these figures show that upon increasing the salt concentration, the screening electrostatic contribution, the attraction between two macroions increases, even though no direct macroion−macroion dispersion force is included.

Figures 8 and 9 compare the mean force between two macroions with size and charge corresponding to hen-egg-white lysozyme proteins at pH 4.5 in monovalent electrolytes of ionic strength 0.2 M for NaCl, NaI, and NaSCN. As the protein (macroion) is positively charged, the anions are the counterions. Results from Monte Carlo simulations (Figure 8) and from the OZ-HNC integral equation (Figure 9) are in qualitative agreement. Figure 9 shows that the mean force obtained from the OZ-HNC equation is relatively insensitive to ion−protein van der Waals dispersion interactions for distances smaller than

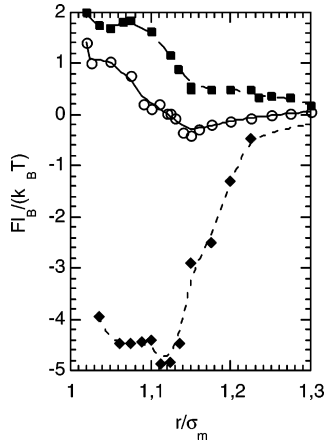

Figure 8. Total mean force (from MC simulations) between two macroions with size and charge corresponding to hen-egg-white lysozyme proteins at pH 4.5 in monovalent electrolytes of ionic strength 0.2 M for NaCl (squares), NaI (circles), and NaSCN (diamonds). (The lines are fitted curves obtained using KaleidaGraph.)

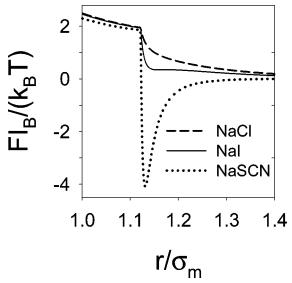

Figure 9. Total mean force between two macroions with size and charge corresponding to hen-egg-white lysozyme proteins at pH 4.5 in monovalent electrolytes of ionic strength 0.2 M for NaCl (squares), NaI (circles), and NaSCN (diamonds). Lines are numerical solutions of the OZ-HNC integral equation.

$1.12\sigma_m$, the minimum separation required to accommodate a monolayer of counterions inbetween the macroions. While in fair agreement with Monte Carlo simulation, the macroion−macroion potentials of mean force obtained from the OZ-HNC equation are not quantitatively reliable, even in the absence of van der Waals interactions. Details concerned with the limitations of the integral equation approaches to highly asymmetric systems, either asymmetry in size or in charge, are reported elsewhere.[21b,22,24,27]

The osmotic second virial coefficient represents a commonly used measure of the strength of protein−protein interactions and provides important information about colloid−solution stability. The second virial coefficient A_2 can be written as a function of the total interaction potential of mean force between two lysozyme particles in solution

$$\frac{MA_2}{v} = \frac{2\pi N_A}{Mv}\int_0^{\infty}\{1 - \exp[U_{tot}(r)/k_BT]\}r^2\, dr \qquad (7)$$

$$U_{tot}(r) = \begin{cases} +\infty & \text{for } r < \sigma_m \\ W(r) - \dfrac{\epsilon}{r^6} & \text{for } r > \sigma_m \end{cases} \qquad (8)$$

Here, M is the molecular weight, and v the partial specific excluded volume (for lysozyme equal to 0.74[6]). With this normalization MA_2/v is equal to 4 for hard spheres. $W(r)$ is the potential of mean force obtained from simulations (described above) devoid of the direct van der Waals interaction between the two globular proteins (Figure 10). As calculation of the

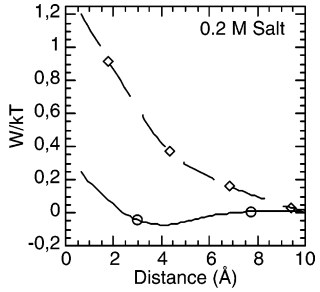

Figure 10. Potential of mean force between two "lysozyme" macroions in a monovalent electrolyte of ionic strength 0.2 M for NaCl (diamonds) and NaI (circles) as a function of surface−surface distance.

second virial coefficient depends on total interprotein interaction, $W(r)$ is supplemented by a direct attractive van der Waals/hydrophobic term ϵr^{-6} ($\epsilon = 8.4 \times 10^9$ kJ/(mol Å^6)) previously shown to accommodate reasonably well the second virial coefficients in lysozyme NaCl solutions. A positive second virial coefficient indicates overall repulsive forces in the colloidal (protein) solution. The solution is more likely to crystallize when the overall forces are more attractive , i.e., the more negative the second virial coefficient becomes. We find that the normalized second virial coefficient of lysozyme is around −0.8 in 0.2 M NaCl and below −5 in 0.2 M NaI. The compressibility obtained from the structure factor is related to the osmotic pressure and hence with the second virial coefficient. This enables a direct comparison of our theoretical results with those extracted from small-angle X-ray scattering. Bonneté et al.[21] deduced $MA_2/v = -0.78$ for 0.2 M NaCl at 20 °C (prepared with a 50 mM NaOAc buffer at pH 4.5, which should give a net protein charge near our model protein). The normalized second virial coefficient became more attractive with increasing salt concentration (increased screening) and with increasing polarizability of the ions.

VII. Conclusions

We compared results for spatial ion−macroion correlations and for the macroion−macroion potential of mean force in aqueous solutions of ionized globular proteins obtained from the nonlinear Poisson−Boltzmann equation with those from Monte Carlo simulations and from the Ornstein−Zernike hypernetted chain integral equation. We showed that the Poisson−Boltzmann equation provides a surprisingly accurate description of the co-ion and counterion concentrations near a charged protein. A Monte Carlo procedure,[14,15] applied to a model with ion−ion and ion−protein dispersion interactions,[10] was used to estimate the osmotic second virial coefficient of lysozyme in simple electrolyte solutions. It is evident that the inclusion of nonelectrostatic (dispersion) potentials can account, at least qualitatively, for the observed ion-specific trends. While it is clear that rigorous studies of ion-speciffic effects require the inclusion of molecular solvent interactions, our results indicate that the van der Waals ion−macroion interactions represent a major and possibly the dominant contribution to the observed salt dependence. Planned future work will explore how other nonelectrostatic contributions may contribute to the effective potential of mean force between pairs of nanoscale colloidal particles.

Acknowledgment. M.B. thanks the Swedish Research Council for financial support and computer time. F.W.T. thanks the CNPq and Capes, the Brazilian agencies, for financial support. D.B. acknowledges support from the National Science Foundation through award BES-0432625.

References and Notes

(1) Curtis, R. A.; Ulrich, J.; Montaser, A.; Prausnitz, J. M.; Blanch, H. W. *Biotechnol. Bioeng.* **2002**, *79*, 367.
(2) Kunz, W.; Lo Nostro, P.; Ninham, B. W. *Curr. Opin. Colloid Interface Sci.* **2004**, *9*, 1.
(3) Franks, G. *J. Colloid Interface Sci.* **2002**, *249*, 44.
(4) Kunz, W.; Henle, J.; Ninham, B. W. *Curr. Opin. Colloid Interface Sci.* **2004**, *9*, 19.
(5) Ries, M. M.; Ducruix, A. F. *J. Biol. Chem.* **1989**, *264*, 745. Carbonnaux, C.; Ries-Kautt, M.; Ducruix, A. *Protein Sci.* **1995**, *4*, 2123.
(6) Finet, S.; Skouri-Panet, F.; Casselyn, M.; Bonnete, F.; Tardieu, A *Curr. Opin. Colloid Interface Sci.* **2004**, *9*, 112 and references therein.
(7) Ninham, B. W.; Yaminsky, V. *Langmuir* **1997**, *13*, 2097.
(8) (a) Boström, M.; Williams, D.; Ninham, B. W. *Langmuir* **2001**, *17*, 4475. (b) Boström, M.; Ninham, B. W. *Langmuir* **2004**, *20*, 7569. (c) Boström, M.; Kunz, W.; Ninham, B. W. *Langmuir* **2005**, *21*, 2619.
(9) (a) Boström, M.; Williams, D. R. M.; Ninham B. W. *Phys. Rev. Lett.* **2001**, *87*, 168103. (b) Boström, M.; Tavares, F. W.; Finet, S.; Skouri-Panet, F.; Tardieu, A.; Ninham, B. W. *Biophys. Chem.* **2005**, *117*, 217.
(10) Tavares, F. W.; Bratko, D.; Blanch, H.; Prausnitz, J. M. *J. Phys. Chem. B* **2004**, *108*, 9228. Tavares, F. W.; Bratko, D.; Prausnitz, J. M. *Curr. Opin. Colloid Interface Sci.* **2004**, *9*, 81.
(11) Boström, M.; Williams, D. R. M.; Ninham, B. W. *Biophys. J.* **2003**, *85*, 686.
(12) Boström M.; Craig, V.; Albion, R.; Williams, D.; Ninham, B. W. *J. Phys. Chem. B* **2003**, *107*, 2875.
(13) Jönsson, B.; Wennerström, H.; Halle, B. *J. Phys. Chem.* **1980**, *84*, 2179.
(14) (a) Bratko, D.; Jönsson, B.; Wennerström, H. *Chem. Phys. Lett.* **1986**, *128*, 449. (b) Linse, P. *J. Phys. Chem.* **1986**, *90*, 6821. (c) Israelachvili, J. N. *Intermolecular and Surface Forces*; Academic Press: London, 1992.
(15) Wu, J.; Bratko, D.; Prausnitz, J. M. *Proc. Natl. Acad. Sci. U.S.A.* **1998**, *95*, 15169.
(16) Wu, J.; Bratko; D.; Blanch H. W.; Prausnitz, J. M. *J. Chem. Phys.* **1999**, *111*, 7084.
(17) (a) Bratko, D.; Vlachy, V. *Chem. Phys. Lett.* **1982**, *90*, 434. Bratko, D.; Vlachy, V. *Chem. Phys. Lett.* **1985**, *115*, 294. (b) Das, T.; Bhuiyan, L. B.; Bratko, D.; Outhwaite, C. W. *J. Phys. Chem.* **1995** *99*, 410.
(18) Sanchez-Sanchez, J. E.; Lozada-Cassou, M. *Chem Phys. Lett.* **1992**, *190*, 202.
(19) Guldbrand, L.; Jönsson, B.; Wennerstrom, H.; Linse, P. *J. Chem. Phys.* **1984** *80*, 2221.
(20) (a) Carlsson, F.; Malmsten, M.; Linse, P. *J. Phys. Chem. B* **2001**, *105*, 12189. (b) Bhuiyan, L. B.; Bratko D.; Outhwaite, C. W. *J. Phys. Chem.* **1991**, *95*, 336.
(21) (a) Bonneté, F.; Finet, S.; Tardieu, A. *J. Cryst. Growth* **1999**, *196*, 403. (b) Belloni, L. *Chem. Phys.* **1985** *99*, 43.
(22) Bratko, D.; Friedman, H. L.; Zhong, E. C. *J. Chem. Phys.* **1986**, *85*, 377.
(23) Bratko, D.; Friedman, H. L.; Chen, S. H.; Blum, L. *Phys. Rev A* **1986**, *34*, 2215.
(24) Bratko, D.; Sheu, E. Y.; Chen, S. H. *Phys. Rev. A* **1987**, *35*, 4359.
(25) (a) Bratko, D.; Wang, D.; Chen, S. H. *Chem. Phys. Lett.* **1990**, *163*, 239. (b) Bratko, D.; Henderson, D. *Electrochim. Acta* **1991**, *36*, 1757.
(26) Rossky, P. J.; Dale, W. D. T. *J. Chem. Phys.* **1980**, *73*, 2457.
(27) Friedman, H. L. *A Course in Statistical Mechanics*; Prentice-Hall: Englewood Cliffs, NJ, 1985.